2011 2nd International Conference on Environmental Science and Development
IPCBEE vol.4 (2011) © (2011) IACSIT Press, Singapore

2D width-averaged numerical simulation of density current in a diverging channel

Mitra Javan
Department of civil Engineering
Razi University, Assistant Professor
Kermanshah, Iran
e-mail: javanmi@gmail.com

Afshin Eghbalzadeh
Department of civil Engineering
Razi University, Assistant Professor
Kermanshah, Iran
e-mail: afeghbal@yahoo.com

Abstract— **When a buoyant inflow of higher density enters a reservoir, it sinks below the ambient water and forms an underflow. Downstream of the plunge point, the flow becomes progressively diluted due to the fluid entrainment. This study seeks to explore the ability of 2D width-averaged unsteady Reynolds-averaged Navier-Stokes (RANS) simulation approach for resolving density currents in an inclined diverging channel. A 2D width-averaged unsteady RANS equations closed by a buoyancy-modified $k-\varepsilon$ turbulence model are integrated in time with a second-order fractional step approach coupled with a direct implicit method and discretized in space on a staggered mesh using a second-order accurate finite volume approach incorporating a high resolution semi-Lagrangian technique for the convective terms. A series of 2D width-averaged unsteady simulations are carried out for density currents. Comparisons with the experimental measurements and the other numerical simulations show that the predictions of velocity and density field are with reasonable accuracy.**

Keywords; width-averaged, unsteady RANS, density currents, diverging channel

I. INTRODUCTION

When a river enters the relatively quiescent water of a lake or reservoir, it meets waters of slightly different temperature, salinity, or turbidity. Three configurations may occur. First, if the river is lighter than the surface water, it will form an overflow. Such a current has been observed in Lake Kootenay in Canada [1]. Second, if the river reaches a depth where its density equals that of the ambient lake water, the plume separates from the bottom and spreads horizontally along surfaces of constant density [2]. Third, when the river is heavier than the water of the lake, it sinks and flows as an inclined plume along its morphological channel. For instance, such a current has been reported by Hebbert et al. (1979) in the Wellington Reservoir in Australia [3]. The analysis of density currents is of great relevance for water quality management in reservoirs as they carry suspended matters and dissolved solids across the lake. Consequently, density currents often determine the distribution of pollutant substances in lakes. Several laboratory experiments have been performed to study density currents. Some studies have essentially dealt with inclined channels of constant width [4-5] and the others have been considered channels of variable widths [6] or unbounded 3D plumes [7]. With the rapid development of numerical methods and advancements in computer technology, CFD has been widely used to study density currents. Unsteady RANS approach with the statistical turbulence model provides a viable alternative for engineering computations of gravity currents at Practical Reynolds numbers and several such models have been proposed in the literature. The $k-\varepsilon$ two-equation model has been widely adopted by researchers to simulate 2D conservative gravity currents with constant width channels [7-11]. Bournet et al. (1999) simulated plunging gravity currents in an inclined channel of constant width and then in a diverging channel [12]. The commercially available code PHOENICS was used for calculations by Bournet et al. (1999). Simulations were presented after the head of the current has passed and the undercurrent reaches steady state. Plunging flow is intrinsically unsteady because of continuous entrainment of ambient water [11]. On the other hand, existing commercial codes have some limitations. For instance, the memory requirements and execution time are often excessive for solving hydraulic engineering problems. The CFD software is also very expensive. It is beneficial to develop and validate a new numerical model that can speedily solve the specific problems in hydraulic engineering. In this paper, the model employing the Boussinesq form of the width-averaged unsteady RANS equations in conjunction with a buoyancy-extended $k-\varepsilon$ closure for the turbulence [13] is developed for unsteady simulation of density currents in an inclined diverging channel. We carry out numerical simulations of various continuous density currents in an inclined diverging channel and then the numerical results are compared with the experimental measurements and the numerical simulation published by Johnson and Stefan (1988) and Bournet et al. (1999), respectively [14,12]. We also present the 2D width-averaged numerical simulation of the density current in an inclined diverging channel at selected time instants.

II. GOVERNING EQUATIONS

In this study we focus on flows with relatively small density differences for which the usual Boussinesq approximation can be assumed to be valid—i.e. all variations in density can be neglected except for the buoyancy term. Incorporating the Boussinesq hypothesis to relate the Reynolds stresses with the mean rate of strain tensor via an eddy viscosity, 2D width-averaged unsteady RANS equations for incompressible, stratified flow read as:

$$\frac{\partial B\widetilde{u}}{\partial x}+\frac{\partial B\widetilde{w}}{\partial z}=0 \tag{1}$$

$$\frac{\partial B\widetilde{u}}{\partial t}+\frac{\partial B\widetilde{u}^2}{\partial x}+\frac{\partial B\widetilde{u}\widetilde{w}}{\partial z}=\frac{-B}{\rho_\circ}\frac{\partial \widetilde{P}^*}{\partial x}+\frac{\partial}{\partial x}\left(2(\nu+\nu_t)B\frac{\partial \widetilde{u}}{\partial x}\right)+\frac{\partial}{\partial z}\left((\nu+\nu_t)B(\frac{\partial \widetilde{u}}{\partial z}+\frac{\partial \widetilde{w}}{\partial x})\right) \tag{2}$$

$$\frac{\partial B\widetilde{w}}{\partial t}+\frac{\partial B\widetilde{w}^2}{\partial z}+\frac{\partial B\widetilde{u}\widetilde{w}}{\partial x}=-\frac{B}{\rho_\circ}\frac{\partial \widetilde{P}^*}{\partial z}+\frac{\partial}{\partial z}\left(2(\nu+\nu_t)B\frac{\partial \widetilde{w}}{\partial z}\right)+\frac{\partial}{\partial x}\left((\nu+\nu_t)B(\frac{\partial \widetilde{u}}{\partial z}+\frac{\partial \widetilde{w}}{\partial x})\right)-\frac{(\rho-\rho_\circ)}{\rho_\circ}gB \tag{3}$$

Where B is the width of channel at x ; $\widetilde{u}$ and $\widetilde{w}$ are the width-averaged velocities along x and z directions, respectively; $\rho_\circ$ is the density of the ambient fluid; g is the acceleration due to gravity; ν and ν_t are the molecular and eddy viscosity, respectively; ρ is the local mixture density and t is time. $\widetilde{P}^*=\widetilde{P}-\rho_\circ g\widetilde{h}$ is the modified width-averaged pressure including the gravity terms where $\widetilde{P}$ is total width-averaged pressure and $\widetilde{h}$ is distance from the reference in z direction. The eddy viscosity is modeled by the buoyancy-modified $k-\varepsilon$ turbulence model as [20]:

$$\nu_t=C_\mu\frac{\widetilde{k}^2}{\widetilde{\varepsilon}} \tag{4}$$

Where $\widetilde{k}$ and $\widetilde{\varepsilon}$ are the width-averaged values of the turbulent kinetic energy and dissipation and C_μ is a model constant. Quantities of $\widetilde{k}$ and $\widetilde{\varepsilon}$ are obtained from the solution of the transport equations:

$$\frac{D\widetilde{k}}{Dt}=\frac{\partial}{\partial x}\left((\nu+\frac{\nu_t}{\sigma_k})B\frac{\partial \widetilde{k}}{\partial x}\right)+\frac{\partial}{\partial z}\left((\nu+\frac{\nu_t}{\sigma_k})B\frac{\partial \widetilde{k}}{\partial z}\right)+B\left(P_r+P_b-\varepsilon\right) \tag{5}$$

$$\frac{D\widetilde{\varepsilon}}{Dt}=\frac{\partial}{\partial x}\left((\nu+\frac{\nu_t}{\sigma_\varepsilon})B\frac{\partial \widetilde{\varepsilon}}{\partial x}\right)+\frac{\partial}{\partial z}\left((\nu+\frac{\nu_t}{\sigma_\varepsilon})B\frac{\partial \widetilde{\varepsilon}}{\partial z}\right)+BC_{\varepsilon1}\frac{\widetilde{\varepsilon}}{\widetilde{k}}\left(P_r+C_{\varepsilon3}P_b\right)-BC_{\varepsilon2}\frac{\widetilde{\varepsilon}^2}{\widetilde{k}} \tag{6}$$

In the above equations, P_r and P_b are production terms of turbulent kinetic energy due to the mean velocity gradient and the buoyancy and are estimated. In above equations, σ_k, σ_ε and σ_t = turbulent Prandtl number for $\widetilde{k}$, $\widetilde{\varepsilon}$ and the source of density current (in this study, width-averaged temperature $\widetilde{S}$), respectively. $C_{\varepsilon1}$, $C_{\varepsilon2}$ and $C_{\varepsilon3}$ are turbulence model constants.

The 2D width-averaged unsteady RANS and turbulence closure equations are solved simultaneously with the following transport equations for the width-averaged temperature $\widetilde{S}$, which is used to determine scalar transport and the variation of the fluid density:

$$\frac{D\widetilde{S}}{Dt}=\frac{\partial}{\partial x}\left((\nu+\frac{\nu_t}{\sigma_t})B\frac{\partial \widetilde{S}}{\partial x}\right)+\frac{\partial}{\partial z}\left((\nu+\frac{\nu_t}{\sigma_t})B\frac{\partial \widetilde{S}}{\partial z}\right) \tag{7}$$

Density is assumed to be linearly related to the mean volumetric concentration through the equation of state as $\widetilde{\rho}=\rho_\circ(1.0+m\widetilde{S})$ where m is a constant.

III. Numerical Method

Non-uniform bathymetry of the computational domains is handled by the sigma-type body-fitted grids which fit the vertical direction of the physical domain. The finite-volume integration method is used for different terms in the governing equations. A fractional step method is employed to integrate the governing equations in time coupled with a projection method for satisfying the continuity equation [15]. The governing equations are discretized in time by fractional-step, or operator splitting, method in which the time advancement is decomposed into a sequence of steps: the advection, the diffusion and the projection. This method allow us deploy the most efficient numerical technique for each of the individual process. Dimensional splitting is also used to reduce the multi-dimensional problem to a series of one-dimensional problems. The fractional step approach for solving the momentum equations is also employed to integrate the transport equations for the turbulence quantities and the temperature. For the later equation only the advection and diffusion steps are required. For the former equations, however, the diffusion step is followed by a step in which the source terms are taken into account explicitly. The discretization of the advection terms in the above iterative scheme is critical for spatial accuracy of the numerical method. We employ the semi-Lagrangian method based on the Fromm scheme (1968) for discretization of the advection terms of the one-dimensional form isolated by the dimensional splitting approach [15-16]. The ULTIMATE conservative difference scheme of Leonard (1991) is employed to ensure to maintain monotonicity while preserving spatial accuracy [17]. The diffusion terms are solved by the semi-implicit second-order Crank-Nicolson scheme to obtain the second intermediate velocity components. During the advection step of the fractional step procedure, the discrete equations are integrated in time explicitly. In the diffusion step the Thomas tri-diagonal matrix algorithm is used to solve the discrete equations implicitly. The pressure-Poisson equation is solved using a block tri-diagonal algorithm, which can be formulated by writing the discrete Poisson equation for all the cells. After calculating the velocity components and pressure field in

new time step, the transport equations for the turbulence kinetic energy, energy dissipation rate and the temperature are solved using the same fractional step algorithm used to integrate the momentum equations. Finally the density is calculated using state equation.

IV. Boundary Conditions

The boundaries of the computational domain are inlet, outlet, free-surface and solid walls. In the absence of wind shear the net fluxes of horizontal momentum and turbulent kinetic energy are set equal to zero at the free surface. Flat, slip boundary condition of zero velocity gradient normal to the surface is applied and the pressure is set equal to the atmospheric value at the surface. The dissipation rate ε is calculated from the relation given by Rodi [13].

The wall function approach is used to specify boundary conditions at the bottom of the channel in order to avoid the resolution of viscous sub-layer [18]. The first grid point of the wall (center of the control volume adjacent to the wall) is placed inside the logarithmic layer based on the buoyancy velocity. At the inlet, known quantities are specified for the inflow velocity, the concentration of the density current source, the current thickness, the turbulent kinetic energy and the dissipation rate. At the outlet the normal gradients of all dependent variables are set equal to zero.

V. Result And Discussion

In this section, we report numerical results for density currents from continuous sources along with comparisons with the experimental and numerical results of Johnson and Stefan and Bournet et al., respectively [14,12]. In Fig. 1, Plan and longitudinal section view of diverging Channel with Sloping Bottom is shown. The Parameters values used in the calculation for the numerical simulation of these cases are summarized in Table I which includes inflow rate (q_0), inlet temperature (T_{inlet}), ambient water temperature (T_0), divergence half-angle of channel (δ), the bottom slope (S), width of inflow channel (B_0) and depth of inflow channel (H_0).

We first present the comparison of the numerical solutions and experimental measurements published by Johnson and Stefan [14]. A 21.8 m long computational domain is employed in order to avoid reflections from the outlet. The calculations have contained 200×30 uniform grids in the *x*- and *z*-direction and a time step of 0.1 second was adopted. We have continued our unsteady simulations until the solutions in the region of interest ($0 \le x \le 6.0\ m$) reach a quasi-equilibrium state. In Fig. 2, the numerical simulation of dimensionless temperature is compared with

TABLE I. The Parameters values for the numerical simulations of the continuous density currents in an inclined diverging channel

Presented by	q_0 (m^3/s)	T_{inlet} $(^\circ C)$	T_0 $(^\circ C)$	δ $(^\circ)$	S ×.001	B_0 (Cm)	H_0 (Cm)
Johnson & Stefan(1988)	0.0018	19.9	39.9	20	52.408	9.1	17
Bournet et al. (1999)	15	10	20	7	25	2000	200

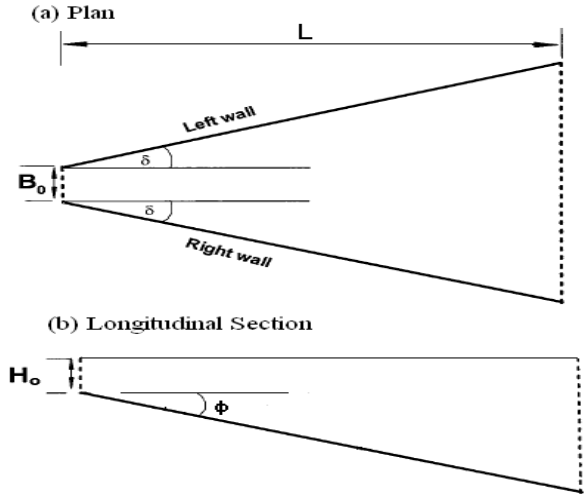

Figure 1. Plan and longitudinal section view of diverging channel with sloping bottom

experimental results of Johnson and Stefan [14] at two sections ($x = 4.2\ m$ and $x = 6.0\ m$) which reveals very good agreement between two sets of results. The dimensionless temperature is expressed in the following:

$$\overline{T} = \frac{T_0 - T}{T_0 - T_{inlet}} \tag{7}$$

Where $\overline{T}$, T_0, T and T_{inlet} are dimensionless temperature, ambient water temperature, temperature and inlet temperature, respectively.

In the second stage, we present the comparison of the numerical solutions and numerical results published by Bournet et al. after the head of the current has passed and the undercurrent reaches steady state [12]. A 5000 m long computational domain is employed in order to avoid reflections from the outlet. The Parameters values used in the calculation for the numerical simulation of this case are summarized in Table I.

In the upstream region of the channel ($0 \le x \le 1500\ m$), calculations have contained 70×20 non-uniform grids in the *x*- and *z*-direction similar to that in [12]. Cells are unevenly spaced, and the grid is squeezed upstream and near the bottom where shear stress occurs and velocity gradients develop. A time step of 0.5 second is adopted. To

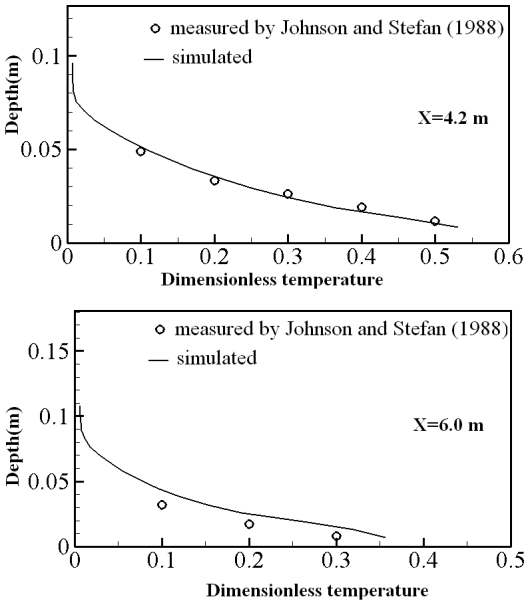

Figure 2. Comparison of simulated dimensionless temperature and experimental results of [14] at two sections

compare numerical solutions with the results of [12], we have continued our unsteady simulations until the solutions in the region of interest ($0 \le x \le 1500\ m$) reach a quasi-equilibrium state. In Figs. 3 and 4, the simulated velocity and temperature field are compared with the results of [12] which reveal very good agreement between two sets of results.

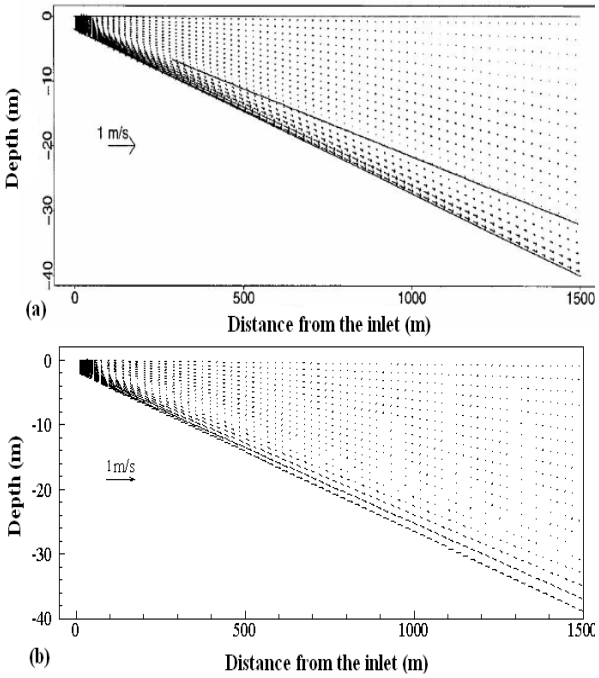

Figure 3. Simulated Velocity Field (a) the results of [12] and (b) the present results

Fig. 5 shows the flow evolution of the density current computed on at several instants in time. Note that the x-axis scales are different in sub-figures of Fig. 5. The numerical solutions reproduce the variation of the longitudinal profile of the density current height and the propagation of the current head. At the first because of dominant inertia force, the total depth of density current is moving forward (Fig. 5, $t = 1\,\text{min}$). At time about 2 minutes, due to dominant buoyancy force, density current plunges to the reservoir bottom and then moves near it. At the plunge point, intense turbulence causes too much mixing of dense fluid and less dense ambient fluid. A dense fluid propagates rightward along the bottom boundary while the ambient fluid moves leftward along the surface boundary naturally due to the density difference. About 5 minutes, density current has been established and then the current head is seen to grow as it travels downstream as dense fluid is pushed by the vortices from the rear part into the head region.

VI. CONCLUSIONS

A series of 2D width-averaged URANS simulations are carried out to resolve continuous density currents in an inclined diverging channel. Comparison of the numerical solutions with available experimental measurements and numerical results leads to the conclusion that 2D width-averaged unsteady RANS simulations using a buoyancy-extended $k-\varepsilon$ turbulence model can resolve reasonably well steady state flow in the rear part. The numerical solutions reproduce the variation of the longitudinal profile of the density current height and the propagation of the current head. Detailed comparisons have shown in general that this two dimensional width-averaged model can be applied to the simulation of the density current in reservoirs which the Froude number of the inlet dense flow and divergence half-angle of reservoir (δ) are less than 2 and 20° , respectively. Although the model presented in this paper is for density current, it can be extended to model two-dimensional turbidity current in an inclined diverging channel. Such a modification is currently being undertaken by the authors.

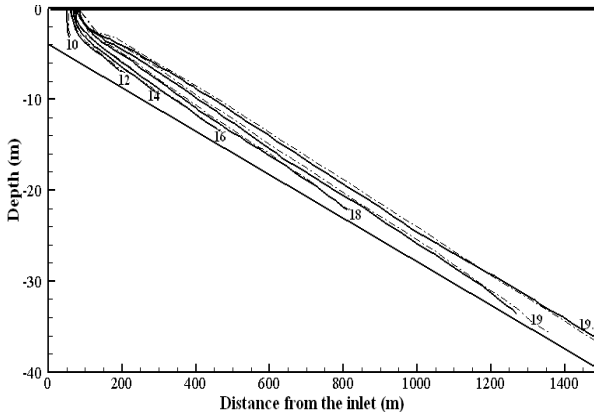

Figure 4. Comparison of simulated iso-contours of temperature distribution (dashed lines) and the results of [12] (solid lines) at a quasi-equilibrium state

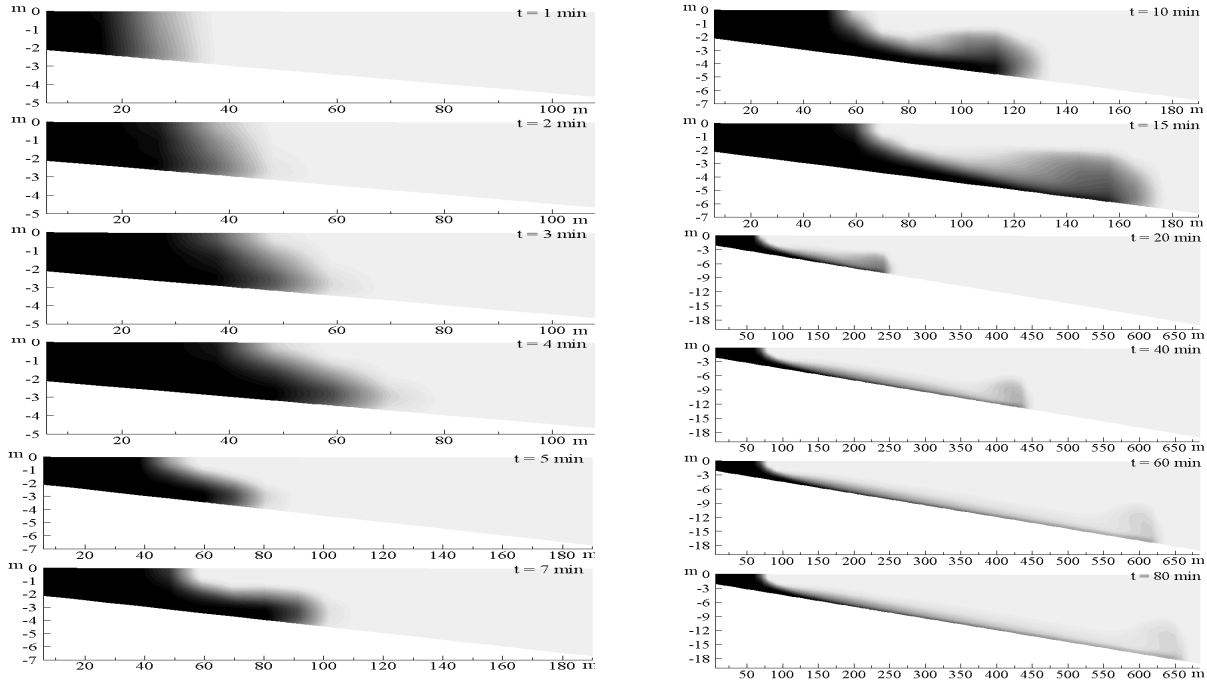

Figure 5. Sequential snapshots of density distributions computed at selected time instants.

REFERENCES

[1] E. C. Carmack , R. C. Wiegand, R. J. Daley, B. J. Gray, S. Jasper, and C. H. Pharo, "Mechanisms influencing the circulation and distribution of water mass in a medium residence-time lake," Limnol.Oceanogr., vol. 31, no. 2, 1986, pp. 249–265.

[2] P. F. Hamblin and E. C.Carmack, ''River induced currents in a fjord lake,'' J. Geophys. Res., vol. 83, no. c2, 1978, pp. 885-899, 83, 885–899, doi:10.1029/JC083iC02p00885.

[3] B. Hebbert, J. Imberger, I. Loh and J. Patterson, "Collie river underflow into the Wellington reservoir," J. Hydr. Div., ASCE, vol. 105, no. 5, 1979, pp. 533-545.

[4] R. A. Denton, "Density current inflows to run of the river reservoirs," Proc., 21st IAHR Congr, 1985.

[5] C. Kranenburg, "Gravity-current fronts advancing into horizontal ambient flow," J. Hydr. Engrg., ASCE, vol. 119, no. 3, 1993, pp. 369-379, doi : 10.1061/(ASCE)0733-9429(1993)119:3(369)

[6] H. G. Stefan, T. R. Johnson, C. R. Ellis, G. J. Farell and J. Akiyama, "Physical limnology, laboratory studies on the initiation of density currents by inflows to lakes and reservoirs," Verhandlungen Internationale Vereinigung für Theoritische und Angewandte Limnologie, Stuttgart, Germany, vol. 23, 1988, pp. 58–61.

[7] V. Alavian, G. H. Jirka, R. A. Denton, M. C. Johnson and H.G. Stefan, "Density currents entering lakes and reservoirs," J. Hydr. Engrg., ASCE, vol. 118, no. 11, 1992, pp. 1464-1489, doi: 10.1061/(ASCE)0733-9429(1992)118:11(1464)

[8] A. Kassem, and J. Imran, ''Three-dimensional modeling of density current. II. Flow in sinuous confined and uncontined channels,'' J. Hydr. Res., vol. 42, issue 6 , 2004 , pp. 591 - 602, doi: 10.1080/00221686.2004.9628313

[9] H. Huang, J. Imran and C. Pirmez, "Numerical model of turbidity currents with a deforming bottom boundary," J. Hydraul. Eng., vol. 131, no. 4, 2005, pp. 283–293, doi: 10.1061/(ASCE)0733-9429(2005)131:4(283)

[10] A. Eghbalzadeh, M. M. Namin, S. A. A. Salehi, B. Firoozabadi and M. Javan, "URANS simulation of 2D continuous and discontinuous gravity currents," J. of Applied Sciences, vol. 8, no. 16, 2008, pp. 2801-2813.

[11] Farrel, G.J. and Stefan, H.G. "Mathematical modeling of plunging reservoir flows," J. Hydraul. Res., vol. 26, issue. 5 , 1988 , pp. 525 – 537, doi: 10.1080/00221688809499191.

[12] P.E. Bournet, D. Dartus, B. Tassin and B. Vincon-Leite, "Numerical investigation of plunging density current," J. Hydraul. Eng., vol. 125, no. 6, 1999, pp.584-594, doi: 10.1061/(ASCE)0733-9429(1999)125:6(584)

[13] W. Rodi, Turbulence models and their applications in hydraulics-a state-of-arts review. IAHR Monograph, Balkema, Rotterdam, The Netherlands, 1993.

[14] T.R. Johnson and H.G. Stefan, "Experimental study of density induced plunging flow into reservoirs and coastal regions," Proj. Rep. No. 245, St. Anthony Falls Hydr. Lab., Univ. of Minnesota, Minneapolis,1988.

[15] M. M. Namin, A Fully Three-Dimensional non-Hydrostatic Free Surface Flow Model for Hydro-Environmental Predictions. PhD thesis, Cardiff School of Engineering, Cardiff University, Cardiff, U.K., 2003.

[16] J. E. Fromm, "A method of reducing dispersion in convective difference schemes," J. of Computational Physics, vol. 3, issue 2, 1968, pp. 176–189, doi: 10.1016/0021-9991(68)90015-6

[17] B. P. Leonard, "The ULTIMATE conservative difference scheme applied to unsteady one-dimensional advection," Computer Methods in Applied Mechanics and Engineering, vol. 88, issue 1, 1991, pp. 17-74,

[18] W. Wu, W. Rodi and T. Wenka, "3D numerical modeling of flow and sediment transport in open channels," J. of Hydraulic Engineering, vol. 126, no. 1, 2000, pp. 4–15, doi: 10.1061/(ASCE)0733-9429(2000)126:1(4)